This paper is published as part of a PCCP Themed Issue on:
Coarse-grained modeling of soft condensed matter

Guest Editor: Roland Faller (UC Davis)

Editorial

Perspective

Communication

Papers

Effective control of the transport coefficients of a coarse-grained liquid and polymer models using the dissipative particle dynamics and Lowe–Andersen equations of motion

Hu-Jun Qian,*[a] Chee Chin Liew[b] and Florian Müller-Plathe[a]

Received 7th October 2008, Accepted 13th November 2008
First published as an Advance Article on the web 8th January 2009
DOI: 10.1039/b817584e

The dynamics of coarse-grained models obtained through iterative Boltzmann inversion [*J. Comput. Chem.*, 2003, **24**, 1624] is always faster than that of the parent atomistic models. In this work, the dissipative particle dynamics (DPD) and Lowe–Andersen (LA) equations of motion are applied in coarse-grained simulations to slow down the coarse-grained dynamics. Both methods provide effective friction and both conserve the linear momentum locally, so that they can be used for the calculation of viscosities. Coarse-grained models of liquid ethylbenzene and of short-chain polystyrene melts are studied. Based on the simulation of ethylbenzene at four different temperatures, empirical rules are proposed for choosing the noise strength in DPD or the bath collision frequency in LA dynamics to reproduce the diffusion coefficients of the fully atomistic simulation. The rules developed using the ethylbenzene system are finally tested on the polystyrene melt where they lead to a close reproduction of the experimental diffusion coefficient.

I. Introduction

The broad span of time and length scales in biosystems and materials is a challenge for computer simulation and modelling. A crucial issue is how to describe and simulate properties or phenomena on scales which are not accessible to straightforward fully atomistic molecular-dynamics (MD) or Monte-Carlo simulations. In recent years, multiscale methods have been developed to overcome this problem. They provide rigorous connections between atomistic models and so-called mesoscale or coarse-grained (CG) models. Several such methods and models have been proposed.[1–17] A book edited by Voth[1] explores recent developments in the fields and explains how the coarse-graining approach can be used in the simulation and modelling of condensed phase and biomolecular systems. In CG simulations, several local atomistic degrees of freedom are averaged out by collecting groups of atoms into CG beads or superatoms. A typical level of coarse graining involves 5–20 atoms per bead. This gives rise to a model which is simpler and computationally more efficient than the fully atomistic model. It is, however, not generic, but retains some of the chemical identity of the system being modelled. *Via* coarse graining, properties can be studied especially for polymeric systems, which are too expensive for atomistic simulations, such as thermodynamic, dynamical, and rheological properties. Thus, CG models are establishing themselves as tools in polymer simulation, which open the possibility of relaxing melts or solutions of high molecular weight polymers and calculating their properties.

In coarse graining, a large number of degrees of freedom are eliminated. The reduced model cannot be expected to reproduce all properties of the system as well as the atomistic model. In selecting a certain CG model, one therefore has to decide which properties it should reproduce to which accuracy. The current CG schemes for polymers are almost exclusively tailored to reproduce the structure of the polymer: bond-length and bond-angle distributions and pair correlation function between nonbonded superatoms. They have done this with remarkable success.[5] Even some thermodynamic quantities could be included as targets into the coarse graining protocol.[6] These CG models, however, tend to show a dynamics which is inherently much too fast, compared either to the parent atomistic model or to experiment. Diffusion coefficients can be too high by 1–2 orders of magnitude and viscosities too low by a similar amount. As an example, we have developed temperature transferable CG models for liquid ethylbenzene (EB) and atactic polystyrene (PS) melts by using the structure-based iterative Boltzmann inversion (IBI) method,[18] where one CG bead represents one EB molecule or one PS repeating unit and is centered on the center of mass of the respective species. In MD simulations, the mobilities are much higher in the CG models than in the corresponding atomistic models (see below). For a previously developed CG model of PS melts,[8] which used a similar mapping scheme (also one bead per chemical repeating unit, but located at a different point) but the same IBI method, the CG dynamics was found to be even 200 times faster than the atomistic or experimental one.

There is some evidence, however, that a lower degree of coarse graining improves the agreement between CG and atomistic models. Harmandaris and co-workers developed two CG models for PS melts[12,19] by using two different mapping schemes, both with two CG beads representing one

[a] *Eduard-Zintl-Institut für Anorganische und Physikalische Chemie, Technische Universität Darmstadt, Petersenstrasse 20, D-64287 Darmstadt, Germany. E-mail: h.qian@theo.chemie.tu-darmstadt.de; Fax: 49 6151 166526; Tel: 49 6151 166537*
[b] *Polymer Research, BASF SE, D-67056 Ludwigshafen, Germany*

PS monomer. They found the CG dynamics measured by the chain diffusion coefficient to be only 8–12 times faster than the atomistic dynamics. Another important issue is the temperature dependence of overestimation of the dynamics by CG models. Simulations of polyamide-6,6 carried out in our group indicate that it decreases with temperature.[17]

These qualitative findings support a possible reason for the increased dynamics of CG models, which has been speculated about for some time: The faster CG dynamics comes from the reduction of the friction between corresponding objects. The reduction of the friction is a consequence of the CG potentials being "softer" than atomistic potentials: a styrene monomer represented by a single convex spherical superatom has a smoother excluded-volume surface than the same monomer described by 16 atoms with their individual exclusion spheres, which combine to form a topography with gaps and protrusions. The fact that a PS model with 2 superatoms per repeating unit has a slower dynamics than a model with 1 superatom per monomer, fits this explanation. Similarly, the decrease of the difference between atomistic and CG mobility with temperature is explained: at high temperature, small details of the potential surface for the interaction between two objects become less important, as the kinetic energy averages them out. Their hard-core repulsion dominates the picture, which is not very different for atomistic and CG models.

We have made a few attempts of generating CG potentials for polymers, which include dynamic properties like viscosity or diffusion coefficient already in the parameterisation procedure. This had previously been done successfully for thermodynamic properties like the density; and CG potentials can be found which simultaneously reproduce the polymer structure and its density.[5,6,18] With dynamic properties we have not been nearly as successful: it appears to be difficult, if not impossible, to find a CG potential which describes both the structure and diffusion of a polymer with equal accuracy.

We therefore propose a different route in this contribution. As the CG potential seems to allow no flexibility for slowing down the dynamics, we turn to the equations of motion. The most straightforward is molecular dynamics (Newton's equations of motion), which we have used in our previous CG simulations[18] mostly together with the Berendsen thermostat.[20] Molecular dynamics allows no tuning of effective frictions to change the dynamics. In its microcanonical form, it is Galilean invariant, conserves the momentum locally, and thus preserves hydrodynamic interactions (HI). These properties are, however, partially lost if MD is used with the Berendsen thermostat, as well as many other common thermostats. If the violation of local momentum conservation is too large (for example, in Brownian dynamics), it will preclude the calculation of viscosities.

Both disadvantages are removed in dissipative particle dynamics (DPD).[21] In addition to the systematic (conservative) force, there is a friction (dissipative) force which can be used to tune the intrinsic particle mobility. It is compensated by a random force.[21] The last two forces are coupled to each other to act as a thermostat according to the fluctuation dissipation theorem.[22] As friction and random forces are applied to pairs of close particles, the DPD equations of motion conserve the local momentum of system, are Galilean invariant and preserve HI. It is important to note that the DPD equations of motion (pairwise dissipative and random forces) are independent of the conservative forces. They can be used as a general-purpose MD thermostat with any type of interaction potential, such as Lennard-Jones type interactions.[23] The disadvantage of DPD is a possible lack of robustness for temperature control when large time steps and strong coupling to the temperature bath (strong dissipative and random forces) are needed.

This possible shortcoming can be altogether avoided in an alternative approach to DPD,[24] the so called Lowe–Andersen (LA) equations of motion, which combines concepts from the Andersen thermostat and DPD.[24] It provides very good temperature control even at large timesteps. In Andersen's original thermostat, the temperature of the system is controlled by resampling the velocities of individual particles from a Maxwell distribution at certain intervals. Thus, it preserves neither the local momentum nor HI. Borrowing the idea from DPD of intervening in the motion of close pairs of particles, the LA resets the velocities of two nearby particles simultaneously, which receive Maxwell-distributed velocities of like magnitude and opposite direction. The forces arising from each momentum reset ("collisions" with imaginary particles of a temperature bath) are central and pairwise, so that the local linear and angular momentum are conserved. Also the LA equations of motion are local, Galilean invariant, and they preserve HI. The viscosity of a fluid simultated with the LA thermostat is proportional to the reset (bath collision) frequency. More frequent bath collision cause a higher viscosity.[24] Besides the problems of frequent discontinuities in the analysis of trajectories, there may be a disadvantage when strong thermostatting (a high collision frequency) is needed in some cases. This situation can be improved by a new Galilean-invariant Nosé–Hoover–Lowe–Andersen (NHLA) thermostat[25] proposed recently by Stoyanov and Groot, where a combination of pairwise Nosé–Hoover and Lowe–Andersen steps is used. The NHLA thermostat has a greater flexibility in adjusting the diffusion coefficient and viscosity of the simulated system. However, in the framework of this paper, the aim is to slow down the too fast dynamics of CG models, rather than thermostatting under difficult circumstances. Therefore, only the LA technique is used.

It has been shown that the faster dynamics in a united-atom model coarse grained from the single-point-charge water model can be effectively controlled and reproduced using the adjusted DPD friction, and the effects of the functional form and the magnitude of the DPD friction on the transport properties have been investigated.[26] Another study, however, of a reduced repulsive Lennard-Jones (LJ) fluid reported that the DPD equation of motion is not capable of controlling the fluid transport properties.[27,28] A possible reason for such contradictory results is the number of neighboring atoms in the interaction range. In the LJ fluid, there are only $\sim$4 atoms within the cutoff sphere of the central atom, whereas there are many more (6–70, depending on the cutoff chosen) neighboring particles in the united-atom water fluid.

In this study, we implement both the DPD and the LA equations of motion for simulations of coarse-grained models of liquid ethylbenzene and of polystyrene melts. The

effectiveness of the two methods is compared and practical rules are proposed for choosing the friction parameter (and noise level) in DPD or the bath collision frequency in LA.

II. Simulation methods and models

a) Dissipative particle dynamics (DPD)

In conventional DPD simulations, particles at a distance R_{ij} interact with each other by three forces, a conservative force $\boldsymbol{F}_{ij}^{C}$, a dissipative force $\boldsymbol{F}_{ij}^{D}$, and a random force $\boldsymbol{F}_{ij}^{R}$. They take the following forms,[21]

$$\boldsymbol{F}_{ij}^{C} = \alpha_{ij}\,(1 - R_{ij}/R_C)\boldsymbol{e}_{ij} \quad (1)$$

$$\boldsymbol{F}_{ij}^{D} = -\gamma w^{D}\,(R_{ij})(\boldsymbol{v}_{ij}\cdot\boldsymbol{e}_{ij})\,\boldsymbol{e}_{ij} \quad (2)$$

$$\boldsymbol{F}_{ij}^{D} = \sigma w^{R}\,(R_{ij})\theta_{ij}\,\Delta t^{-1/2}\,\boldsymbol{e}_{ij} \quad (3)$$

where $\boldsymbol{e}_{ij} = \boldsymbol{r}_{ij}/R_{ij}$ is the unit vector, α_{ij} is interaction strength, γ (kg s^{-1}) and σ (N $s^{1/2}$) are the strengths of dissipative force and random forces, respectively, $w^{D}(R)$ and $w^{R}(R)$ are weighting functions for these forces; θ_{ij} is a uniformly distributed random variable with zero mean and unit variance, which is independent for different pairs of particles and different times.[21,29] In our coarse-grained model, the conservative force (eqn (1)) is replaced by more complex interactions. We keep, however, the DPD equations of motion given by the dissipative and the random force (eqns (2) and (3)). The dissipative force is proportional to the relative velocity of the interacting particle pair, which mimics the friction between particles and accounts for energy dissipation, while the random force compensates for the degrees of freedom removed by coarse graining and acts as a heat source. According to the fluctuation dissipation theorem,[22] the dissipative and random forces are coupled by the relations $w^{D}(R) = [w^{R}(R)]^2 = w(R) = (1-R/R_C)^2$ and $\sigma^2 = 2\gamma k_B T$. Together, they form a thermostat of temperature T.[21] Since noise and friction are coupled, only one of the parameters can be adjusted independently. In our simulations, the noise strength σ is varied. Dissipative and random forces act only between particles within a cutoff radius of R_C. Their pairwise nature together with the short cutoff ensures local momentum conservation leading to correct long-range hydrodynamics.[30]

To solve the stochastic equations of motion we use a modified velocity-Verlet algorithm:[21]

$$\begin{aligned}
&\boldsymbol{r}_i(t+\Delta t) = \boldsymbol{r}_i(t) + \Delta t\boldsymbol{v}_i(t) + \frac{1}{2}(\Delta t)^2\boldsymbol{F}_i(t)/m_i\\
&\tilde{\boldsymbol{v}}_i(t+\Delta t) = \boldsymbol{v}_i(t) + \lambda\Delta t\boldsymbol{F}_i(t)/m_i\\
&\boldsymbol{F}_i(t+\Delta t) = \boldsymbol{F}_i(\boldsymbol{r}(t+\Delta t),\ \tilde{\boldsymbol{v}}(t+\Delta t))\\
&\boldsymbol{v}_i(t+\Delta t) = \boldsymbol{v}_i(t) + \frac{1}{2}\Delta t(\boldsymbol{F}_i(t) + \boldsymbol{F}_i(t+\Delta t))/m_i,
\end{aligned} \quad (4)$$

where an intermediate velocity $\tilde{\boldsymbol{v}}$ is predicted for the calculation of dissipative forces (eqn (2)). The particle velocities are updated in the last step. $\boldsymbol{F}_i$ is the total force on particle i including the non-bonded and bonded forces of the CG force field, the dissipative and the random forces. The empirical integration constant λ is chosen to be 0.65 according to ref. 21.

b) Lowe–Andersen (LA) equations of motion

The Lowe–Andersen technique[24] is an alternative to DPD based on the idea of Andersen's thermostat. It also conserves local linear momentum. Instead of using explicit friction and noise as in DPD, the relative energy of particle pairs within a certain cutoff is dissipated by being periodically resampled from a Maxwell–Boltzmann distribution with a chosen "bath collision" frequency. This is done by adding random velocities along the connecting line between the particles

$$\begin{aligned}
\boldsymbol{v}_i &= \boldsymbol{v}_i + M_{ij}[\xi_{ij}\sqrt{kT_0/M_{ij}} - \boldsymbol{v}_{ij}\cdot\boldsymbol{e}_{ij}]\boldsymbol{e}_{ij}/m_i\\
\boldsymbol{v}_j &= \boldsymbol{v}_j - M_{ij}[\xi_{ij}\sqrt{kT_0/M_{ij}} - \boldsymbol{v}_{ij}\cdot\boldsymbol{e}_{ij}]\boldsymbol{e}_{ij}/m_j,
\end{aligned} \quad (5)$$

where $M_{ij} = m_i m_j/(m_i + m_j)$ is the reduced mass of the particle pair; $\boldsymbol{v}_{ij} = \boldsymbol{v}_i - \boldsymbol{v}_j$ is their relative velocity; $\boldsymbol{e}_{ij}$ is the unit vector along the connecting line; m_i and m_j are the masses of particles i and j, respectively; ξ_{ij} is a Gaussian random variable of zero mean and unit variance generated by an algorithm from ref. 31. By construction, the total momentum of the particle pair is conserved, therefore LA is also locally momentum-conserving and Galilei-invariant.

The interaction with the heat bath is, in LA, described by a Langevin equation for relative velocities rather explicit random and friction forces. As there is no velocity-dependent dissipative force, the equations of motion can be solved by a standard velocity-Verlet algorithm as used in literature[24,32] or the leap-frog scheme which we will use in this study. In every time step, for each pair of close particles a new relative velocity is generated from a Maxwell distribution $\xi_{ij}\sqrt{kT_0/M_{ij}}$ with a probability $\Gamma/\Delta t$ (ps^{-1}). The newly generated relative velocity acts along the connecting line between the particles' centres (eqn (5)). The scheme is, in detail:

(i) $\boldsymbol{F}_i(t) = \boldsymbol{F}_i(\boldsymbol{r}(t))$

(ii) For all pairs of particles for which $R_{ij}(t) < R_C$

(a) Generate $\xi_{ij}\sqrt{kT_0/M_{ij}}$ from a Maxwell distribution with a probability $\Gamma/\Delta t$

(b) $\boldsymbol{v}_i = \boldsymbol{v}_i + M_{ij}[\xi_{ij}\sqrt{kT_0/M_{ij}} - \boldsymbol{v}_{ij}\cdot\boldsymbol{e}_{ij}]\boldsymbol{e}_{ij}/m_i$

(c) $\boldsymbol{v}_j = \boldsymbol{v}_j - M_{ij}[\xi_{ij}\sqrt{kT_0/M_{ij}} - \boldsymbol{v}_{ij}\cdot\boldsymbol{e}_{ij}]\boldsymbol{e}_{ij}/m_j$

(iii) $\boldsymbol{v}_i\left(t+\frac{\Delta t}{2}\right) = \boldsymbol{v}_i\left(t-\frac{\Delta t}{2}\right) + \Delta t\frac{\boldsymbol{f}_i(t)}{m_i}$

(iv) $\boldsymbol{r}_i(t+\Delta t) = \boldsymbol{r}_i(t) + \Delta t\boldsymbol{v}_i\left(t+\frac{\Delta t}{2}\right)$ (6)

The probability $\Gamma/\Delta t$ corresponds to a collision frequency which is controlled by uniform random numbers $u \in (0,1)$. This random number is independent for different particle pairs and different times. For every close pair of particles ($R_{ij}(t) < R_C$), a random number u smaller than preset value of Γ will cause a new relative velocity from a Maxwell distribution to be assigned to the particles.

c) Effect of DPD and LA on transport properties

It has been shown that both DPD and LA dynamics can enhance the effective viscosity of a system, as both the dissipative forces and the collisions provide friction to the particles.

For DPD, Marsh and coworkers[33,34] have shown theoretically that there are two contributions to the shear viscosity: the so-called kinetic part η_K is due to the motion of the particles, the so-called dissipative part η_D arises from momentum transport due to the interactions between particles.

$$\eta = \eta_K + \eta_D = \frac{1}{2} n k_B T_0 \left\{ \frac{1}{\omega_0} + \frac{\omega_0 t_w^2}{d+2} \right\} \qquad (7)$$

where k_B is the Boltzmann constant, T_0 is the bath temperature, $\omega_0 = \gamma n[w]/d$ is the characteristic kinetic relaxation rate, γ is the friction constant of eqn (2), n is the number density with the system size measured in units of the interaction range R_C, $[w] = \int d\mathbf{r}_{ij}\, w(R_{ij})$ is the effective volume of the action sphere, $w(R_{ij})$ is the weighting function of eqn (2), and d is the number of dimensions. The viscosity depends on the two intrinsic time scales: the characteristic kinetic relaxation time, $t_0 = 1/\omega_0 \sim 1/\gamma n$, and the traversal time of the action sphere t_w, defined through $t_w^2 = \langle R_{ij}^2 \rangle_w / \bar{v}^2$ with $\bar{v} = (k_B T_0/m)^{1/2}$ the thermal velocity, and where $\langle R_{ij}^2 \rangle_w = [R_{ij}^2\, w]/[w]$ is of the order of R_C^2. In the parameter range $t_w > t_0$, the dissipative viscosity η_D dominates, and in the range $t_w < t_0$ the kinetic viscosity η_K does.

In LA dynamics,[24] the relative velocity is dissipated by collisions with the particles of the heat bath. The contribution to the viscosity from the collisions in one timestep has been estimated to be $\eta = \pi m n^2 (\Gamma \Delta t^{-1}) R_C^5/75$, which is essentially the same as η_D in eqn (7) apart from a prefactor and the collision frequency $\Gamma/\Delta t$ replacing the friction constant γ. Thus, the collision frequency is the control parameter by which the dynamics of the system can be tuned.

d) Coarse-grained models and simulation details

All the simulations of this paper are carried out based on the temperature-transferable CG models of liquid ethylbenzene (EB) and of melts polystyrene decamers (PS), which have been optimised by the iterative Boltzmann inversion (IBI) method. The details of the two models are reported in ref. 18. Here, we give only a brief summary. The coarse-grained EB molecule is represented by a single bead centered on the real centre of mass. Similarly, one CG bead for one PS monomer is centered on its centre of mass. To represent tacticity, two different bead types (*R* and *S*) are defined according to the absolute configuration of the monomer given by the asymmetric –CHR– group against the given direction of the carbon backbone. Therefore, there are two different non-bonded interactions, *RR* (or the equivalent *SS*) and *RS* (or *SR*); two types of bonds, *R*-*R* (or *S*-*S*) and *R*-*S* (or *S*-*R*); three types of angles, *R*-*R*-*R* (or *S*-*S*-*S*), *R*-*R*-*S* (or *S*-*S*-*R*,*R*-*S*-*S* and *S*-*R*-*R*), and *R*-*S*-*R* (or *S*-*R*-*S*).

The simulations in this work are carried out by using the IBISCO code,[35] which is able to handle tabulated numerical potentials. The DPD and LA equations of motion have been implemented into IBISCO for this study. The non-bonded interactions are truncated beyond R_C = 1.6 nm with a neighbor list cutoff of 1.7 nm. The interaction range of dissipative and random forces in DPD and for bath collision in LA is also set to 1.6 nm. The timestep is 5 fs for both EB and PS throughout the paper unless noted otherwise. The nonbonded interactions between first and second neighbors along the PS chain are excluded. The simulations are carried out at four different temperatures for EB, and at 500 K for the PS decamer melt. Details about the systems are listed in Table 1. In this table, we report the diffusion coefficients from atomistic simulation for the EB system[18] or from experiment for PS melt,[36] the values are used as targets for the coarse-grained DPD and LA simulations. The diffusion coefficients from CG simulations[18] using Newton's equations of motion (MD) together with Berendsen's thermostat are also reported for all systems. Details of the coarse-grained and atomistic MD simulations can be found in our previous work.[18]

The diffusion coefficients D are calculated from the centre-of-mass mean square displacement, using the Einstein relation, $6Dt = \lim_{t\to\infty} \langle |r(t) - r(0)|^2 \rangle$. To check possible effects of the Berendsen thermostat on the diffusion coefficient, we have calculated D from both mirocanonical NVE and Berendsen NVT simulations. For the coarse-grained ethylbenzene model at 298 K both conditions give the same diffusion coefficients to within the error bars: $D^{NVT} = 15.2 \times 10^{-5}$ cm^2 s^{-1} and $D^{NVE} = 16.8 \times 10^{-5}$ cm^2 s^{-1}. The small difference comes from the deviation of the temperature in the NVE simulation, which is slightly higher than 298 K.

III. Results and discussion

An important feature of DPD and LA is the good temperature control as a thermostat. The DPD simulation, however, can result in large temperature deviations when too large time

Table 1 Systems simulated in this study. All results for the density and the diffusion coefficients are obtained in *NPT* simulations from our previous work[18] except the target diffusion coefficient of the PS melt. ϕ is the time scaling factor defined as the ratio between diffusion coefficients from coarse-grained MD simulation using the Berendsen thermostat ($D^{CG\ MD}$) and the target diffusion coefficient (D^{target})[a]

System	Temperature/K	No. of molecules	Density/kg m^{-3}	$D^{target a}/\times 10^{-5}$ cm^2 s^{-1}	$D^{CG\ MD}/\times 10^{-5}$ cm^2 s^{-1}	ϕ
EB	238	200	913	0.32	11.1	34.6
EB	298	200	853	1.35	15.2	11.3
EB	340	200	811	2.61	19.6	7.5
EB	380	200	774	4.22	22.3	5.3
PS10	500	48	942	0.05	1.70	34

[a] The target diffusion coefficient is calculated from atomistic simulations[18] for EB, and estimated from the viscosity by using the Stokes–Einstein relation for the PS decamer melt[8].

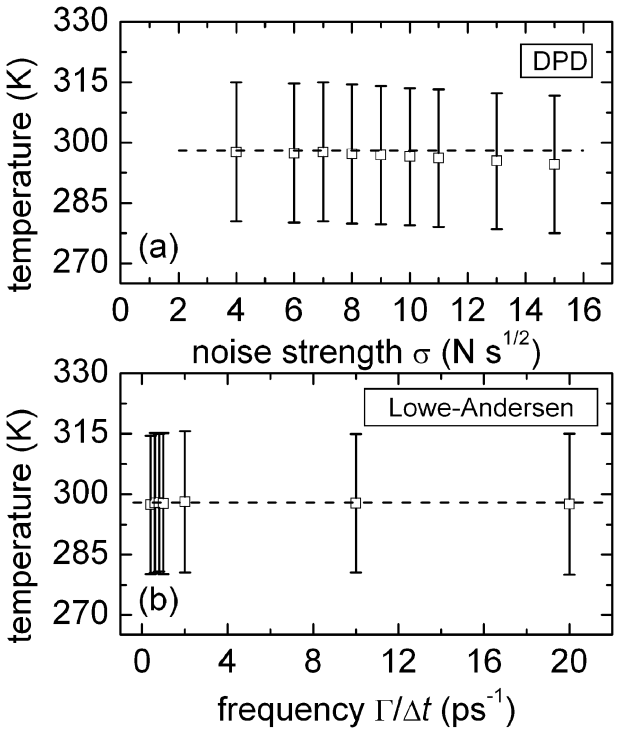

Fig. 1 Temperature maintenance of (a) the dissipative particle dynamics and (b) the Lowe–Andersen thermostat. Simulations are carried out for liquid ethylbenzene at a bath temperature of 298 K (horizontal line). The error bars show the temperature fluctuations.

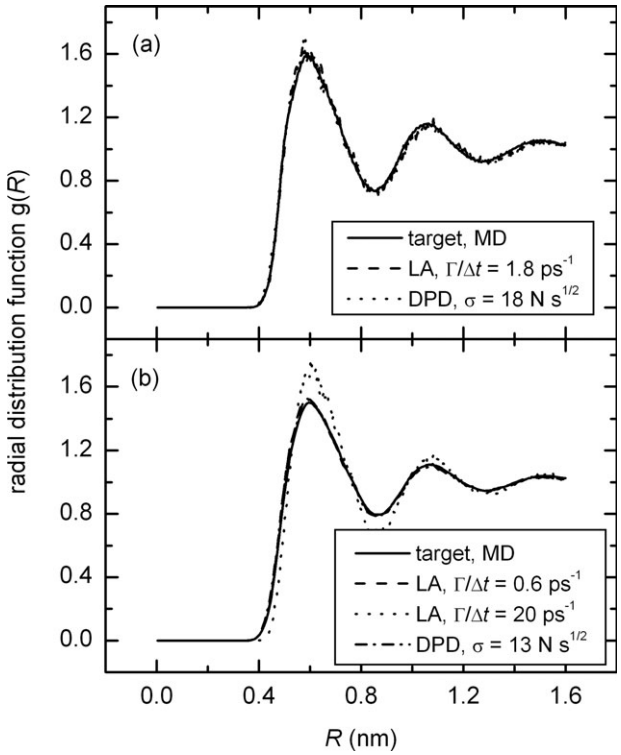

Fig. 2 Radial distribution functions $g(R)$ for ethylbenzene at (a) 238 K and (b) 298 K calculated from coarse-grained simulations using dissipative particle dynamics and Lowe–Andersen (different strengths) dynamics. The target $g(R)$ from atomistic MD simulation is shown for comparison (solid line).

steps or strong noise terms are used. This is attributed to the artefacts of the integrator due to the velocity dependence of the dissipative force.[29,37] This effect can be removed by using the LA technique where no explicit velocity dependent forces are included. A comparison of the effect of the time step on the temperature control in DPD and LA has been reported in ref. 32. In this work, we have studied the ability of the two thermostats to impose the desired target temperature, in order to establish the regime where the methods can be safely used. The time step is fixed at 5 fs and the temperature is shown as a function of the noise strength σ (DPD) and bath collision frequency $\Gamma/\Delta t$ (LA), Fig. 1. It is obvious that in DPD (Fig. 1a), the temperature develops a deviation from the bath temperature 298 K with strong frictions, although it still falls well within the temperature fluctuations. In contrast, the LA thermostat provides a very good temperature control even with frequent bath collisions (Fig. 1b).

Although the main object of the this study is to establish a way of slowing down the too fast dynamics of CG simulations by using DPD and LA equations of motion, it must be ensured that the structure of the system is not disturbed. In Fig. 2(a) and (b), we report the radial distribution functions of coarse-grained ethylbenzene at 238 and 298 K, respectively, calculated both with DPD and LA together with the reference distributions from MD simulation (atomistic and coarse-grained radial distribution functions are identical by construction). With proper friction in DPD and bath collision frequency in LA, the system has the same structure as in MD simulation. In the parameter range of interest the target structure is maintained. For example, when $\sigma = 18$ N s$^{1/2}$ or $\Gamma/\Delta t = 1.8$ ps^{-1} at 238 K, and $\sigma = 13$ N s$^{1/2}$ or $\Gamma/\Delta t = 0.6$ ps^{-1} at 298 K, which results in the same diffusion coefficient as in atomistic MD simulation (see below), the structure of the system is the same as the reference structure. Only for very high bath collision frequencies ($\Gamma/\Delta t = 20$ ps^{-1} in Fig. 2b)), the fluid is more structured due to local cages which are formed by strong friction between neighboring particles.

In Table 1, we report the diffusion coefficients from coarse-grained MD simulations using Berendsen's thermostat and compare them with atomistic MD results or experiment: The diffusion in the CG models is much faster than in the atomistic or experimental reference. To relate the dynamical results of the CG models to reality, one has to find a time scaling factor to match the CG dynamical properties, such as diffusion coefficient[8] or viscosity[38] to the atomistic values. In this study, the time scaling factor ϕ is calculated as the ratio of the CG MD diffusion coefficient and the target diffusion coefficient:

$$\phi = \frac{D^{\mathrm{CG,\,MD}}}{D^{\mathrm{target}}} \qquad (8)$$

D^{target} is calculated from atomistic MD simulation for EB and from experiment for PS as listed in Table 1. In the EB system, ϕ decreases with temperature. A similar decrease of ϕ with temperature has been found for a CG model of polyamide-66.[16] For the PS melt at 500 K, ϕ is 34. *En passant*, we note that this is much smaller than $\phi = 200$ in the previous CG model of PS.[8,38]

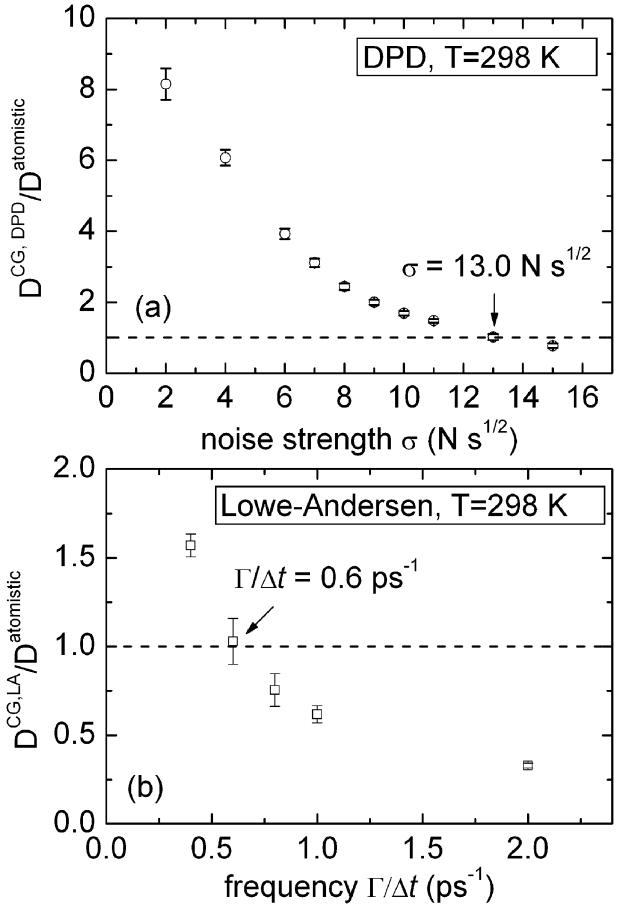

Fig. 3 Diffusion coefficients calculated from simulations with (a) dissipative particle dynamics (DPD) and (b) Lowe–Andersen (LA) thermostats as a function of the noise strength σ in DPD or bath collision frequency in LA. The diffusion coefficient is normalized (divided) by the target value from atomistic simulation.

In order to reproduce the diffusion coefficient of atomistic simulations, the values of σ in DPD and γ in LA are varied manually in the CG simulation of EB. For instance, the results at 298 K are plotted in Fig. 3(a) and (b) for the DPD or LA equations of motion, respectively. The resulting CG diffusion coefficient is divided by the target value. The diffusion coefficient decreases with both the noise strength σ in DPD and the collision frequency $\Gamma/\Delta t$ in LA. When the DPD noise strength σ is 13.0 N $s^{1/2}$, the diffusion coefficient from atomistic simulations is well reproduced (Fig. 3a). The appropriate LA collision frequency $\Gamma/\Delta t$ is 0.6 ps^{-1}. For EB at four different temperatures, the appropriate values of σ and $\Gamma/\Delta t$ have been empirically determined in the same way. They are reported in Table 2 together with the target diffusion coefficients from atomistic simulations. The optimised values of both control parameters (σ and $\Gamma/\Delta t$) are found to decrease exponentially with the temperature. Least squares fits yield:

$$\sigma[\mathrm{N\,s^{1/2}}] = 171.4\exp\left(-\frac{T}{83.2\,\mathrm{K}}\right) + 8.2 \qquad (9)$$

$$\frac{\Gamma}{\Delta t}[\mathrm{ps^{-1}}] = 603.5\exp\left(-\frac{T}{39.8\mathrm{K}}\right) + 0.27 \qquad (10)$$

The empirical eqns (9) and (10) give the rules to choose the DPD and LA control parameters for simulation at different temperatures. They are restricted, however, to the simulation of ethylbenzene. The question arises whether general rules can be found for selecting σ and $\Gamma/\Delta t$ in an *a priori* fashion also for other systems. The appropriate value of the control parameters must be in some implicit way linked to the number of degrees of freedom removed during coarse graining or to the molecular roughness lost in the process. Both are difficult to quantify. For devising and testing a rule, we turn instead to the empirical time scaling factor ϕ, which is the ratio of the dynamical speed (as given by the diffusion coefficient or the viscosity or maybe some other dynamical quantity) between the coarse-grained model and the parent atomistic model or the experiment.

Every selection of a noise strength σ or a collision frequency $\Gamma/\Delta t$, respectively, for the coarse-grained model leads to a characteristic dynamical "speed" of the system which may be measured with reference to the speed of the coarse-grained model in molecular dynamics. If diffusion coefficients are used to describe the speed of the system, the relative speed is given by a second time scaling factor $\Phi = D^{\mathrm{CG,MD}}/D^{\mathrm{CG,DPD}}$ or $\Phi = D^{\mathrm{CG,MD}}/D^{\mathrm{CG,LA}}$, respectively. This time scale factor depends on the choice of σ or $\Gamma/\Delta t$. (Once σ or $\Gamma/\Delta t$ has been optimised for the DPD or LA calculation of the coarse-grained model to reproduce the diffusion coefficient of atomistic MD, Φ of course becomes identical to ϕ.)

The relation between the chosen σ (or $\Gamma/\Delta t$) and the resulting value of Φ has been empirically determined for ethylbenzene at 298 K. The data points are shown in Fig. 4 for σ in DPD (Fig. 4a, open circles) and $\Gamma/\Delta t$ in LA (Fig. 4b, open triangles), respectively. Least-squares fits to these points give the following relations:

$$\sigma[\mathrm{N\ s^{1/2}}] = 7.243\,(\Phi - 0.886)^{0.35} - 3.393 \qquad (11)$$

$$\frac{\Gamma}{\Delta t}[\mathrm{ps^{-1}}] = -6.022\times10^{-2} + 5.974\times10^{-2}\Phi \qquad (12)$$

Both equations satisfy the limit of the atomistic simulations: the time scaling factor Φ becomes 1, no external friction or

Table 2 Calculated diffusion coefficients of ethylbenzene at different temperatures both with DPD and Lowe–Andersen dynamics. Appropriate control parameters (σ in DPD, $\Gamma/\Delta t$ in LA dynamics) are listed, too. Reference diffusion coefficients from atomistic MD simulations[18] (D^{target}) are listed as targets for comparison

Temperature/K	$D^{\mathrm{target}}/\times10^{-5}$ cm^2 s^{-1}	σ/N s$^{1/2}$	$D^{\mathrm{CG,\ DPD}}/\times10^{-5}$ cm^2 s^{-1}	$\Gamma/\Delta t$/ps^{-1}	$D^{\mathrm{CG,LA}}/\times10^{-5}$ cm^2 s^{-1}
238	0.32	18	0.36	1.8	0.30
298	1.35	13	1.39	0.6	1.37
340	2.61	11	2.60	0.4	2.53
380	4.22	10	4.24	0.3	4.12

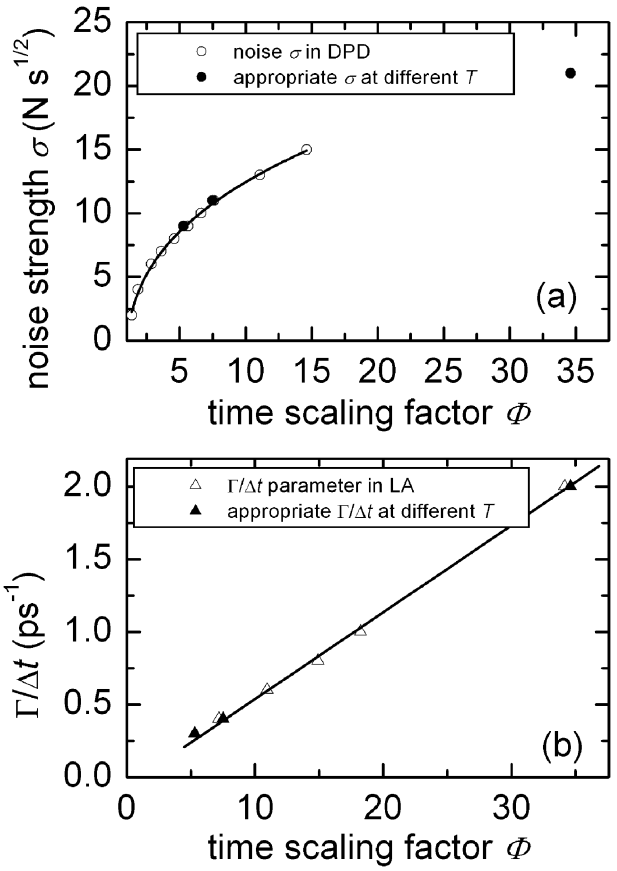

Fig. 4 Values of the control parameters (a) σ (open circles) in dissipative particle dynamics and (b) $\Gamma/\Delta t$ (open triangles) in Lowe–Andersen (LA) dynamics, plotted *versus* the corresponding time scaling factor Φ obtained from the simulation of ethylbenzene (EB) at 298 K. The optimised control parameters for EB at three different temperatures (238, 340, and 380 K) are also shown (solid symbols).

bath collisions are needed, and both the σ and $\Gamma/\Delta t$ parameters become zero. More encouragingly, the optimised control parameters (σ and $\Gamma/\Delta t$), which reproduce the true EB diffusion coefficients at three different temperatures (238, 340, and 380 K), are also described by these relations. The corresponding points fall well onto the curves in Fig. 4 (solid symbols), indicating a transferability of the rules (eqns (11) and (12)) to other temperatures.

For different systems, different time scaling factors ϕ (the ratio of the dynamical speed between the CG MD model and the parent atomistic model or the experiment) will result. Even for the same system, different coarse graining schemes or coarse graining levels may result in different time scaling factors.[8,18,19] All the detailed atomistic information removed during coarse graining affects the time scaling factor. The above eqns (11) and (12) indicate relations between the effect of removed degrees of freedom on the dynamics (as described by the time scaling factor) and the amount of friction which needs to be introduced to compensate for this effect. To test whether or not eqns (11) and (12) are system-independent, and whether they provide general rules for choosing the appropriate values of the control parameters (σ and $\Gamma/\Delta t$) also for different systems, the PS melt at 500 K (time scaling factor ϕ = 34, Table 1) is simulated with the DPD and LA equations of motion. The appropriate σ parameter for DPD inferred from eqn (11) is 21 N $s^{1/2}$, and the proper bath collision frequency $\Gamma/\Delta t$ for LA from eqn (12) is 2.0 ps^{-1}. The centre-of-mass diffusion coefficients of PS calculated with these control parameters come close to the reference value: the DPD diffusion coefficient is $D^{CG,DPD} = 8.3 \times 10^{-7}$ cm^2 s^{-1}, which is close to the experimental value 5.0×10^{-7} cm^2 s^{-1}. In the LA simulation with the rule-based collision frequency $\Gamma/\Delta t = 2.0$ ps^{-1}, a diffusion coefficient $D^{CG,LA} = 4.2 \times 10^{-7}$ cm^2 s^{-1} is obtained, which is almost the same as in the experiment. The good agreement of the coarse-grained PS dynamics by DPD or LA with control parameters inferred from the empirical rules (eqns (11) and (12)) is encouraging. It is, at the moment, not clear whether this success is a mere coincidence, whether it arises from the similarity of the two systems (ethylbenzene is, after all, a close approximation to a polystyrene repeating unit), or whether the rules can be generalised. A preliminary application of these rules to the coarse-grained model of an ionic liquid has been successful.[39] Further case studies will be carried out in the future.

IV. Conclusions

We have used the dissipative particle dynamics and Lowe–Andersen equations of motion to simulate coarse-grained models of a liquid (ethylbenzene) and a short-chain polymer melt (decamer of polystyrene). The coarse-grained potentials were generated from atomistic reference simulations and are solely structure-based; their parameterisation contains no dynamic information. In straightforward molecular dynamics (Newton's equations of motion with or without a Berendsen thermostat) they produce a dynamics which is much too fast compared to either experiment or atomistic simulations. The overestimation, called time scaling factor ϕ in this paper and defined as the ratio of coarse-grained and atomistic/experimental diffusion coefficients, can reach up to 35. This behaviour has been observed for all coarse-grained models and is due to the neglect of degrees of freedom by coarse graining, the smoothing of the molecular envelope and the ensuing loss of friction between molecules or segments.

Our simulations show that both DPD and LA can re-introduce friction into the system and compensate for the dynamical effects of coarse graining. Thus, the too fast dynamics of CG models in molecular dynamics can be corrected and can be slowed down to match reality. The control parameters are the noise strength σ in DPD and the bath collision frequency $\Gamma/\Delta t$ in LA. For ethylbenzene, we have optimised them manually at four temperatures, until the self-diffusion coefficients matched the atomistic results. We have found empirically that the optimised noise strength σ in DPD follows a power dependence on the time scaling factor ϕ, whereas the optimised bath collision frequency in LA dynamics $\Gamma/\Delta t$ scales linearly with ϕ. The empirical relations (eqns (11) and (12)) allow to select the appropriate values of the control parameters, once the time scaling factor has been gauged.

It is not clear yet, how transferable these rules are among different systems. We have, however, taken the empirical rule derived for ethylbenzene and applied it successfully to find

suitable control parameters for the melt of PS decamers at 500 K. Although calculations on more systems are required to establish how general the rules can be made, this is a promising first test case. Based on the findings of this work, we tentatively suggest the following protocol for calculating the dynamic properties of polymers using multiscale simulation: (i) perform atomistic simulations to obtain structural distributions as well as dynamic or transport properties on small systems such as oligomeric melts. (ii) Use the atomistic structural distributions in iterative Boltzmann inversion to obtain the coarse-grained potential. (iii) Use the dynamic properties from the atomistic and the coarse-grained molecular dynamics calculations to gauge the time scaling factor of the coarse-grained model. (iv) Select the DPD noise strength or the LA collision frequency from the time scaling factor based on the empirical rules (eqns (11) or (12)). (v) Calculate the dynamic properties for the full-size system, for example a long-chain polymer melt, using the coarse-grained model with the DPD or the Lowe–Andersen method.

Acknowledgements

We are grateful for financial support from BASF SE, Ludwigshafen.

References

1 G. A. Voth, *Coarse Graining of Condensed Phase and Biomolecular Systems*, CRS Press, Taylor and Francis Group, 2007.
2 W. Tschöp, K. Kremer, J. Batoulis, T. Bürger and O. Hahn, *Acta Polym.*, 1998, **49**, 61.
3 R. Faller, H. Schmitz, O. Biermann and F. Müller-Plathe, *J. Comput. Chem.*, 1999, **20**, 1009.
4 D. Reith, H. Meyer and F. Müller-Plathe, *Comput. Phys. Commun.*, 2002, **148**, 299.
5 F. Müller-Plathe, *ChemPhysChem*, 2002, **3**, 754.
6 D. Reith, M. Pütz and F. Müller-Plathe, *J. Comput. Chem.*, 2003, **24**, 1624.
7 H. S. Ashbaugh, H. A. Patel, S. K. Kumar and S. Garde, *J. Chem. Phys.*, 2005, **122**, 104908.
8 G. Milano and F. Müller-Plathe, *J. Phys. Chem. B*, 2005, **109**, 18609.
9 G. Milano, S. Goudeau and F. Müller-Plathe, *J. Polym. Sci., Part B: Polym. Phys.*, 2005, **43**, 871.
10 Q. Sun and R. Faller, *Comput. Chem. Eng.*, 2005, **29**, 2380.
11 L.-J. Chen, H.-J. Qian, Z.-Y. Lu, Z.-S. Li and C.-C. Sun, *J. Phys. Chem. B*, 2006, **110**, 24093.
12 V. A. Harmandaris, N. P. Adhikari, N. F. A. van der Vegt and K. Kremer, *Macromolecules*, 2006, **39**, 6708.
13 G. Santangelo, A. di Matteo, F. Müller-Plathe and G. Milano, *J. Phys. Chem. B*, 2007, **111**, 2765.
14 T. Spyriouni, C. Tzoumanekas, D. Theodorou, F. Müller-Plathe and G. Milano, *Macromolecules*, 2007, **40**, 3876.
15 P. Carbone, F. Negri and F. Müller-Plathe, *Macromolecules*, 2007, **40**, 7044.
16 Q. Sun and R. Faller, *Macromolecules*, 2006, **39**, 812.
17 P. Carbone, H. A. K. Varzaneh, X. Chen and F. Müller-Plathe, *J. Chem. Phys.*, 2008, **128**, 064904.
18 H.-J. Qian, P. Carbone, X. Chen, H. A. K. Varzaneh, C. C. Liew and F. Müller-Plathe, *Macromolecules*, 2008, **41**, 9919.
19 V. A. Harmandaris, D. Reith, N. F. A. van der Vegt and K. Kremer, *Macromol. Chem. Phys.*, 2007, **208**, 2109.
20 H. J. C. Berendsen, J. P. M. Postma, W. F. v. Gunsteren, A. DiNola and J. R. Haak, *J. Chem. Phys.*, 1984, **81**, 3684.
21 R. D. Groot and P. B. Warren, *J. Chem. Phys.*, 1997, **107**, 4423.
22 P. Español and P. Warren, *Europhys. Lett.*, 1995, **30**, 191.
23 E. A. Koopman and C. P. Lowe, *J. Chem. Phys.*, 2006, **124**, 204103.
24 C. P. Lowe, *Europhys. Lett.*, 1999, **47**, 145.
25 S. D. Stoyanov and R. D. Groot, *J. Chem. Phys.*, 2005, **122**, 114112.
26 A. Eriksson, M. Nilsson Jacobi, J. Nyström and K. Tunstrøm, *J. Chem. Phys.*, 2008, **129**, 024106.
27 T. Soddemann, B. Dünweg and K. Kremer, *Phys. Rev. E*, 2003, **68**, 046702.
28 C. Junghans, M. Praprotnikab and K. Kremer, *Soft Matter*, 2008, **4**, 156.
29 P. Nikunen, M. Karttunen and I. Vattulainen, *Comput. Phys. Commun.*, 2003, **153**, 407.
30 I. Pagonabarraga, M. H. J. Hagen and D. Frenkel, *Europhys. Lett.*, 1998, **42**, 377.
31 D. Frenkel and B. Smit, *Understanding Molecular Simulation: From Algorithms to Applications*, Academic, Boston, 1996.
32 L.-J. Chen, Z.-Y. Lu, H.-J. Qian, Z.-S. Li and C.-C. Sun, *J. Chem. Phys.*, 2005, **122**, 104907.
33 C. A. Marsh, G. Backx and M. H. Ernst, *Europhys. Lett.*, 1997, **38**, 411.
34 C. A. Marsh, G. Backx and M. H. Ernst, *Phys. Rev. E*, 1997, **56**, 1676.
35 http://www.theo.chemie.tu-darmstadt.de.
36 G. Milano, G. Guerra and F. Müller-Plathe, *Chem. Mater.*, 2002, **14**, 2977.
37 I. Vattulainen, M. Karttunen, G. Besold and J. M. Polson, *J. Chem. Phys.*, 2002, **116**, 3967.
38 X. Chen, P. Carbone, W. L. Cavalcanti, G. Milano and F. Müller-Plathe, *Macromolecules*, 2007, **40**, 8087.
39 H. A. Karimi-Varzaneh, P. Carbone, S. Balasubramanian and F. Müller-Plathe, unpublished.